Transactions of the SMiRT 27
Yokohama, Japan, March 3-8, 2024
Division V

VALIDATION OF NONLINEAR MECHANICAL MODELS FOR NUCLEAR BUILDINGS: APPLICATION TO SMART2013 MOCK-UP

Thomas Langlade[1], Thomas Heitz[1,*], David Bouhjiti[1], Benjamin Richard[1], Alexis Courtois[2], François Voldoire[3]

[1] IRSN/PSN-EXP/SES/LMAPS, B.P. 17 - 92262 Fontenay-aux-Roses Cedex, France
[2] EDF DIPNN/DT, 19, rue Pierre Bourdeix, 69007 Lyon, France
[3] EDF R&D, 7, boulevard Gaspard Monge, 91120 Palaiseau, France
[*] Corresponding author: thomas.heitz@irsn.fr

ABSTRACT

The validation of numerical results of a given model provided for the Safety Margin Assessment (SMA) in the nuclear industry is a crucial task that still relies strongly on the expert's judgement. Most common and available guides and regulatory corpus from recent decades lack a clear, straightforward, and practical method for quantifying the validity of numerical results. This issue becomes more significant when dealing with nonlinear models for which uncertain inputs, strong model's sensitivity to boundary conditions and initial states, or numerical convergence are challenging the users of the finite element software.

Accordingly, IRSN and EDF decided to work within a joint framework to define more precisely the verification and validation (V&V) concepts and their related operational application. This is done in three steps: the first covers a review of the state-of-the-art of current practices both from a regulatory and research points of view; the second deals with the proposition of a comprehensive, practical, and pragmatic methodology agreed upon by IRSN and EDF; the third and last covers several industrial applications aiming at proving the concept and demonstrating the feasibility of the proposed approach.

This paper is a follow-up of the one proposed in SMiRT-26 by Langlade et al. (2022) dealing with the general concepts of V&V thoroughly and applying them to the case of two pounding structures. It focuses on the achieved improvements with regards to the methodology since then and provides a practical application case based on the SMART 2013 RC building mock-up for which extensive experimental results are available under seismic records of increasing intensity. This validation procedure brings useful information to the user of the model such as the uncertainty contributions of the spatial discretization, of the input uncertainties, of the model formulation and mostly of the extrapolation of the model to cases for which no experimental measurements are available (blind analysis). To present these advancements, the paper is divided in three parts. First, a general description of the mock-up and the model is presented. Then, the validation methodology derived from the work of Roy and Oberkampf (2011) is applied. Finally, a discussion is made on possible improvements of the model and future work regarding the validation measuring methods.

INTRODUCTION

Verification and validation are two distinct notions that are essential to judge whether a numerical result is acceptable and reliable. Verification assesses whether a numerical model is in accordance with its theoretical framework, focusing on the acceptability of errors due to numerical implementation and solving. Validation, conversely, assesses if a model correctly reflects experimental observations within acceptable gaps. In other words, validation aims at determining whether a numerical model (and therefore the associated physical hypotheses) correctly reproduces experimental observations, given a precision level defined by the engineer. To do this, the latter should use the output of a reliable and trustworthy software that was already subjected to a verification process. The distinction between the validation cases and the case of interest is crucial. Often, models are validated against scenarios with ample experimental data and then applied to less documented cases. Validation confirms the adequacy of representing both aleatory and epistemic uncertainties in modeling physical phenomena. So, EDF and IRSN have jointly developed a validation flowchart (Figure 1), involving four stages: (1) analysis of experimental tests and mock-up, (2) numerical analysis including modeling and uncertainty identification, (3) computation of validation metrics, and (4) extrapolation of outcomes to untested conditions.

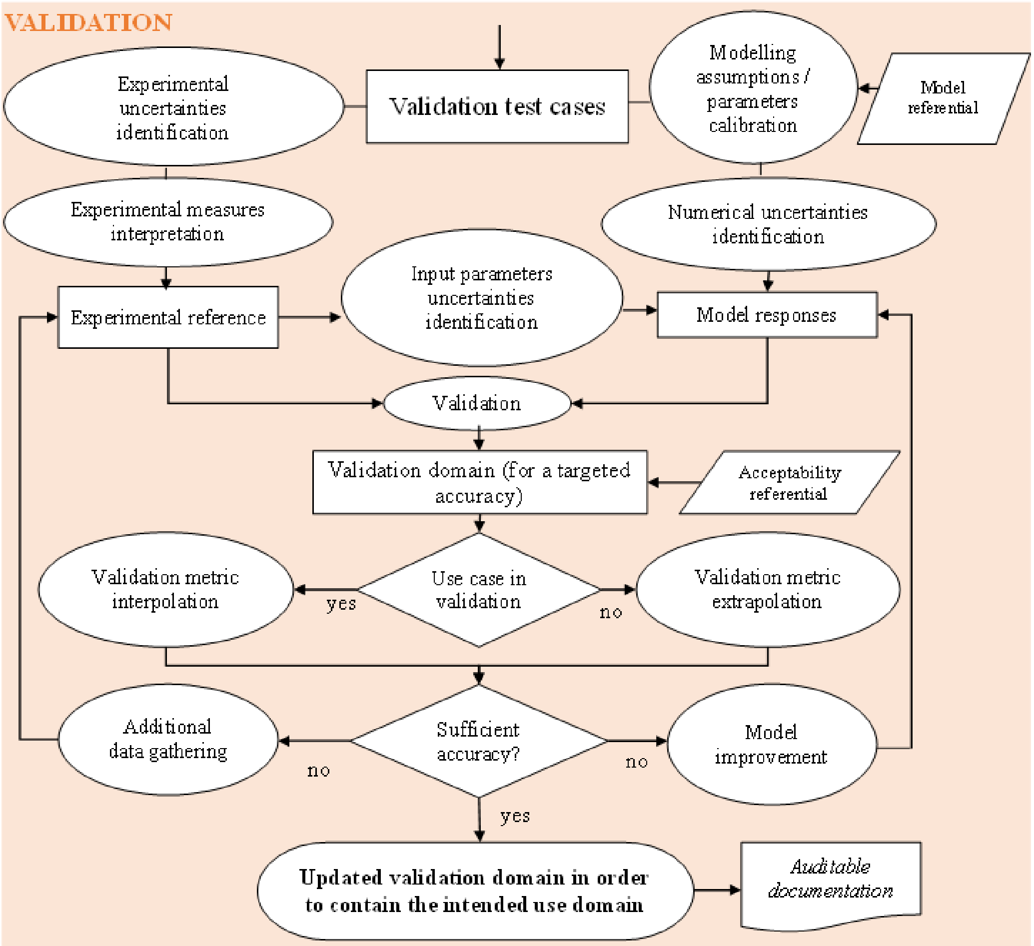

Figure 1. Proposed validation flowchart

In the literature, Roy and Oberkampf (2011) developed a metrics — noted d_0 in this paper — to quantify the agreement between uncertain model outputs and uncertain reference data represented by probability boxes (p-boxes). These p-boxes are the envelope of a collection of (empirical) cumulative distribution functions of the samples. Each curve corresponds to one epistemic sample. This metrics is the measure of the area between both p-boxes, as illustrated for a generic example in blue and red in Figure 2.

The d_0 metrics possesses two key characteristics: it is dimensionally consistent with the variable of interest and represents an unbounded positive real number. However, a notable limitation of the d_0 metrics is its inability to differentiate between overestimation and underestimation errors. This means that a model consistently underestimating the variable of interest could have the same d_0 value as another model that alternates between underestimation and overestimation of the same variable across different scenarios. To address this issue, a new approach is proposed hereafter where sample-related errors are treated as random variables. A sample-related error has the same unit as the Engineering Demand Parameter (EDP) of interest and corresponds to the distance between the experimental and numerical p-boxes for a given probability of exceedance. By doing so, one can get three possible domains (as depicted in Figure 3 for a generic example): (a) the domain of the negative errors where the model underestimates experimental results; (b) a domain of the positive errors where the model overestimates the experimental results; (c) a domain where the model matches experimental results given the considered epistemic and random uncertainties. Then, once this curve identified, specific error quantiles can be selected for a predetermined level of confidence. For example (see Figure 3), there is a 95 % probability that the model's error lies within the range of [-4.63; 3.53]. These values, referred to as $err(2.5\ \%)$ and $err(97.5\ \%)$, are introduced as new metrics to measure the congruence between the model outputs and experimental values for a given intensity measure (IM). It is important to note that these new metrics (plural as it depends on the level of confidence one chooses) are attributed solely to the model, as the effects of uncertainties in the input parameters are already accounted for by using probability boxes (p-boxes). Therefore, a zero error does not indicate a perfect match between the model and the reference data; it suggests instead that the observed discrepancies cannot be solely ascribed to the model's formulation and physical representativeness.

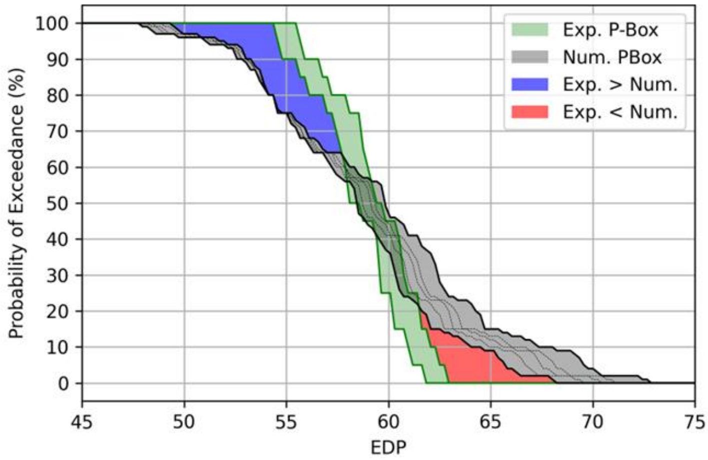

Figure 2. Area between numerical and experimental probability boxes (generic example)

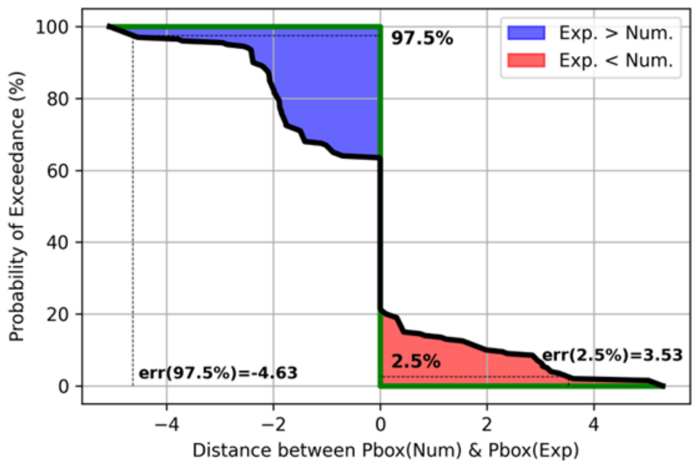

Figure 3. Model vs reference probability boxes errors (generic example)

Then, as done in the work of Roy and Oberkampf (2011), the two metrics $err(2.5\ \%)$ and $err(97.5\ \%)$ can be calculated for various available Intensity Measures (IMs). Following this calculation, these metrics can be further analyzed through extrapolation or interpolation using an adapted regression technique that is not necessarily linear. This additional step of regression introduces a new layer of predictive uncertainty, which can be quantitatively assessed. By incorporating this step, the range over which the model's validation is applicable — known as the validation domain — can be effectively expanded. This expansion comes with the trade-off of introducing additional uncertainties into the model's predictions.

As an illustration, let us consider that the previous err values have been extrapolated to a higher IM, which increases their values (considering both their trend and the additional prediction uncertainties) to -9.69 and 8.29 in the EDP unit. Then, the model is computed at the target IM, and the p-box of the model output for this higher IM (for which no experimental data are available) can be plotted in blue and extended in green accounting for this additional model error, as illustrated in Figure 4. Such a plot is rich in information: one can tell that, at this higher IM, there will be 95 % of probability that the (real) system will exhibit an EDP higher than 104, but lower than 163, from a conservative point of view.

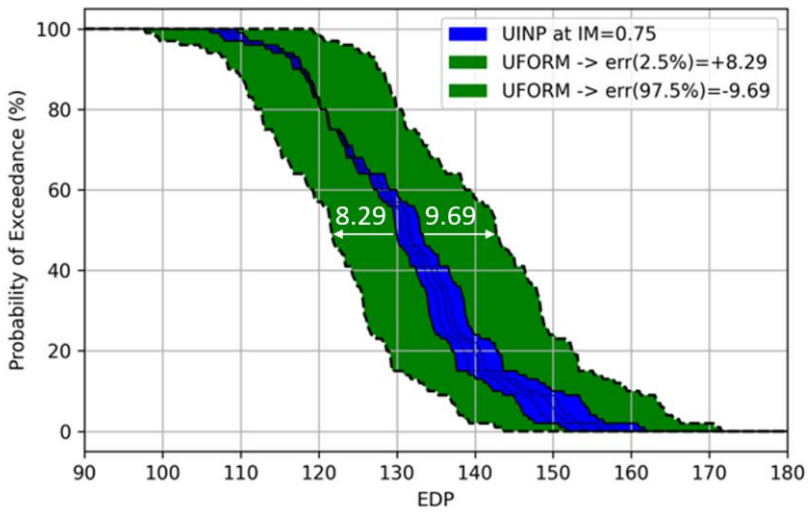

Figure 4. Model output p-box at a higher IM without experimental data (generic example)

To illustrate the use of the flowchart and the proposed validation metrics, it has been applied to a practical case: SMART2013. This refers to an experimental campaign carried out on a 1:4 scale reinforced concrete mock-up representative of a nuclear building subjected to torsion and nonlinear effects under seismic loads. This application work is presented in the following sections and serves as a proof of concept and feasibility prior to an industrial level.

APPLICATION TO SMART2013 MOCK-UP

Overview of the mock-up and the finite elements model

A comprehensive presentation of the mock-up and the experiments can be found in the paper Richard et al. (2018). In few words, SMART2013 is a 3.6-meter-high asymmetric reinforced concrete structure subjected to increasing seismic loads on a laboratory shaking table at CEA (see Figure 5). The mock-up is subjected to bi-axial horizontal seismic loads with three sets of ground motions, namely signal 1: design (synthetic) signal; signal 2: main shock of the Northridge earthquake; signal 3: aftershock of the Northridge earthquake.

The initial measured eigenfrequencies of the structure are 6.28 Hz (bending along X), 7.86 Hz (bending along Y) and 16.50 Hz (torsion along Z). The relative drops in frequencies measured for each eigenmode during the whole experimental campaign were respectively equal to 60 %, 43 % and 48 %. The successive input signals sent to the shaking table are summarized in Table 1. Damage occurred mainly at the base of the model and at the top of the narrower wall (labelled 04) at the 1st level. During run 19 (signal 2: main shock of the Northridge earthquake at 100 % nominal level), significant damage occurred at the end and base of wall #04, resulting in a large crack opening (over 10 mm), presumably because of the failure of the steel covering in this area, without compromising the stability of the mock-up (Figure 6, left). The application of the two aftershock signals (signal 3) did not generate any additional damage. From run 07 to run 23, there were 3 instances where the mock-up significantly showed signs of progressive damage after runs 13, 17, and 19 (see Figure 6, right).

Table 1: Runs applied on SMART2013 mock-up

	Achieved PGA (X/Y)
Run 07: 50 % Design Signal	0.10 g/0.14 g
Run 09: 100 % Design Signal	0.22 g/0.23 g
Run 11: 11 % Northridge Main Shock	0.21 g/0.16 g
Run 13: 22 % Northridge Main Shock	0.40 g/0.25 g
Run 15: 22 % Northridge Main Shock	0.40 g/0.24 g
Run 17: 44 % Northridge Main Shock	0.60 g/0.40 g
Run 19: 100 % Northridge Main Shock	1.10 g/1.00 g
Run 21: 33 % Aftershock Northridge Signal	0.14 g/0.14 g
Run 23: 100 % Aftershock Northridge Signal	0.70 g/0.40 g

Figure 5. SMART2013 mock-up (©CEA).

Figure 6. Crack at the bottom of wall 04 after Northridge 0.40 g (left); final state of SMART2013 (right), Richard et al. (2018)

Numerical model

In this work, two models are considered: one based on linear equivalent method and one using transient nonlinear analysis. Both share the same mesh and boundary conditions detailed in this paper. Figure 7 (left) displays the numerical SMART2013 and shaking table models and axis. The numerical model has been developed using Cast3M finite element software from CEA (2022). It is composed of finite elements of various natures:

- a shaking table model composed of elastic linear shell elements;
- the foundations are elastic linear cubic elements;
- the concrete of walls/slabs/beams are 5-layer-shell elements associated with the RICCOQ constitutive model by Richard and Ragueneau (2012);
- the steel rebars of walls/slabs/beams are 4-layer-shell elements associated with a linear elastic behavior because rebars remained elastic during the various experimental seismic runs;
- for the same reason, the column is modeled using elastic linear multifiber elements.

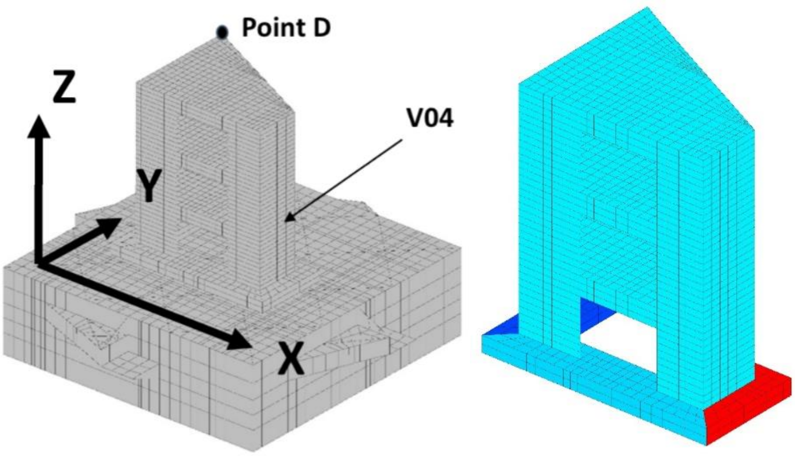

Figure 7. Complete numerical model and control point D of interest (left), SMART2013 numerical model only (right)

Overall, with an average element size of 15 cm, the complete model — including the shaking table — encompasses approximately 62,000 degrees of freedom:

- the inclusion of the shaking table in the FE model is crucial, given its mass (25 tons) relative to the mock-up's mass (46 tons). This inclusion is necessary to accurately account for its contribution to the global dynamical stiffness matrix.
- the foundations are divided into three distinct zones, each visibly differentiated in Figure 6 (right). The Young's Modulus for each zone is adjusted to align with the expected eigenfrequency values. Specifically, the foundations in the dark blue, light blue, and red zones have their Young's Modulus set to 0.86 GPa, 7.09 GPa, and 18.4 GPa, respectively.

  Rayleigh's damping coefficients (ξ_1 and ξ_2) have been calculated to achieve the desired damping level in the range of frequency of interest (between 85 % of the first eigenfrequency and 100 % of the third eigenfrequency).

Only runs 07, 11, 15, 17 and 19 in Table 1 are considered in the following study, providing reference data at increasing PGA levels of 0.10, 0.21, 0.40, 0.60 and 1.10 g along X axis. Aftershock runs 21 and 23 are not computed as they did not induce additional damage to SMART2013. Finally, transient nonlinear solving is limited to runs 15, 17, and 19.

VALIDATION OF THE SMART2013 MODEL

Sensitivity Analysis

A Morris' sensitivity analysis — see for example Herman et al. (2013) or Baudin et al. (2016) for illustration of the method — is performed on the linear version of SMART2013 model. This method known for its computational efficiency is useful for globally assessing how sensitive the EDPs are to variations in input parameters derived from experimental data. While this analysis could potentially be applied to the nonlinear model given sufficient resources, it has not been done in this case. To keep computational cost as reasonable as possible, the element size is arbitrarily set at 0.2 m. The analysis helps identify which parameters most significantly affect the propagation of uncertainties. The parameters examined include Young's modulus, concrete density, element size, number of layers in shell elements, and Rayleigh damping ratios.

The concrete density, the number of concrete layers in the shell elements, and element size have little effects on the drift compared to other material parameters. An additional nonlinear sensitivity analysis would have shown that the concrete tensile strength has also a major impact on the structural drift, as shown by Richard et al. (2018). Consequently, the uncertainties of the Young's modulus, the concrete tensile strength, and the Rayleigh damping ratios are further investigated in the next section, while the other parameters are fixed based on experimental measures and/or expert's knowledge.

Uncertainties Characterization

The first part amongst the four of the validation flowchart described in the introduction has been partially addressed while presenting the mock-up and its model. Within the second part, a crucial task consists in the characterization of the uncertain inputs: epistemic or aleatory nature, type of distribution and the two first statistical moments in the second case.

The selection of Rayleigh damping coefficients is often a subject of discussion, influenced by factors such as modeling choices, constitutive laws, loading intensity, and prevailing norms and guidelines. Based on our experts' judgement, a range for the modal damping ratio has been set between 3% and 6%, reflecting its epistemic uncertainty as illustrated in Figure 9.

The concrete material properties are chosen as the main aleatory uncertainty, namely the Young's modulus E, the tensile resistance f_t, and the fracture energy G_f. These properties are sampled as correlated triplets thanks to a multivariate lognormal quasi-Monte-Carlo sampling to assess the natural correlation between those concrete mechanical properties as observed by Richard et al. (2018). Considering the 5 days computation time for each sample, the total number of samples has been kept relatively low to 30 for the nonlinear model. It was verified that the mean and standard deviation of the samples set reached convergence with 30 triplets to the following values:

- Young's modulus: mean of 25.7 GPa and standard deviation of 1.9 GPa;
- tensile strength: mean of 3.33 MPa and standard deviation of 0.44 MPa;
- fracture energy: mean of 130 J/m² and standard deviation of 8.38 J/m².

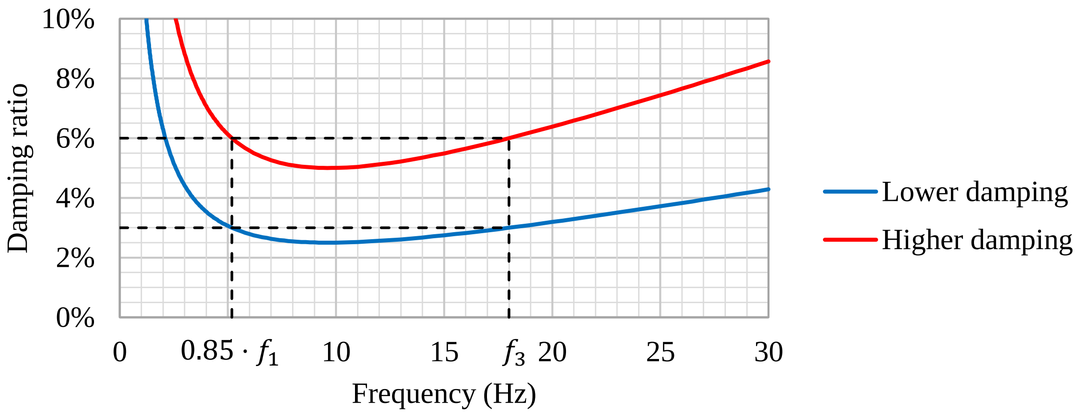

Figure 8. Upper and lower envelopes of the epistemic Rayleigh damping (f_1 and f_3 are the first and third eigenfrequencies)

Validation domain

The previously drawn samples are used as input for both the linear and nonlinear models. The output of interest is the drift of the point D in the X direction (Figure 7, left). The mean and 2-standard deviation interval are plotted in Figure 9.

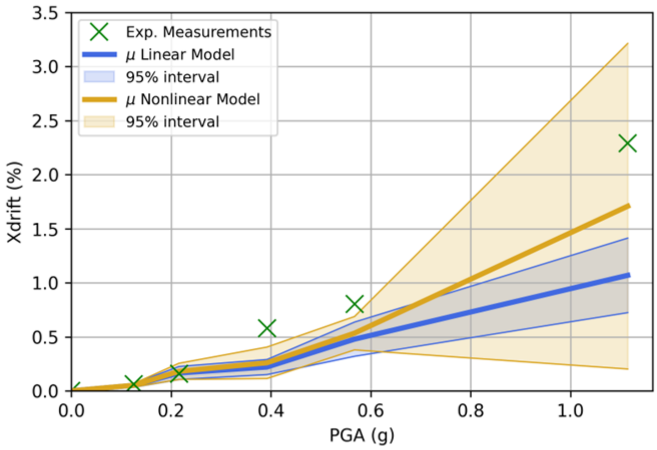

Figure 9. Comparison between linear and nonlinear models

Incorporating nonlinearities into the model results in a noticeable increase in drift, bringing the median curve of the model's output closer to the experimental measurements, especially at higher record intensities. However, this also causes a considerable increase in variability, resulting in a substantial widening of the 95 % confidence envelope. This 95 % interval is calculated based on a normal distribution, using the mean and twice the standard deviation. Notably, at high PGA values, the simulation outputs exhibit significant scatter. This can sometimes be attributed to issues with numerical convergence, leading to a notably broad interval at 1.1 g PGA.

The metrics $err(97.5\ \%)$ and $err(2.5\ \%)$ are calculated for each run within the validation domain, as detailed in the introduction. From these calculations, two distinct linear regression models emerge, with their respective prediction intervals being determined. The highest boundary of the $err(2.5\ \%)$ metrics and the lowest boundary of the $err(97.5\ \%)$ metrics are combined to form a comprehensive error prediction interval, as shown in Figure 10. The immediate outputs from both models are represented as two probability boxes (p-boxes), illustrated in Figure 11. These p-boxes are then adjusted according to the extrapolated err metrics by shifting their upper and lower envelopes, a process depicted in Figure 12. Before this adjustment, at a PGA of 1.78 g — a level beyond the range of the available experimental data — the linear model consistently predicts lower drift values compared to the nonlinear model. Additionally, the outputs from the nonlinear model display greater epistemic uncertainty, indicated by the wider span of its p-box. However, after applying the err metrics correction, this scenario changes. The nonlinear model exhibits less epistemic uncertainty than the linear model, and the linear model's responses become almost identical to those of the nonlinear model, provided the upper envelope (right side) of its p-box is considered. Consequently, the corrected linear model emerges as a potentially valuable and computationally efficient alternative to the more representative nonlinear model for drift estimation at given PGA values.

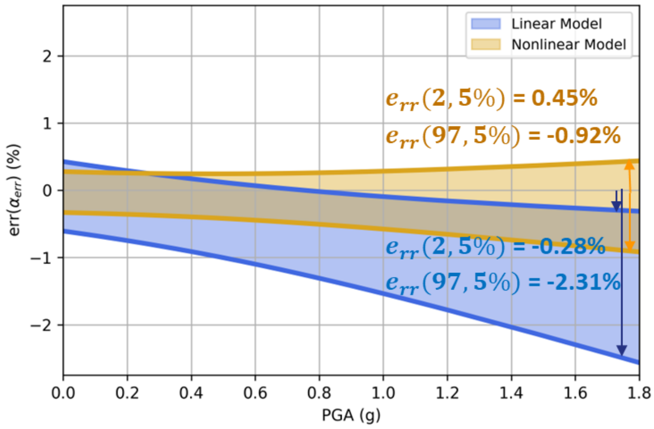

Figure 10. Prediction intervals of err (in drift) for both the linear and nonlinear models of SMART2013

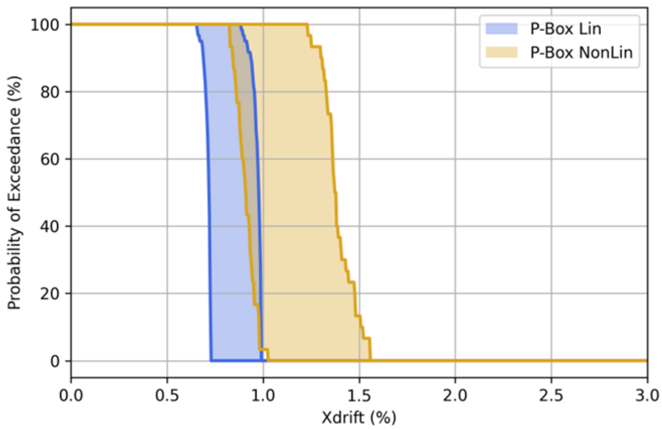

Figure 11. Direct output p-boxes for the linear and nonlinear models of SMART2013 at PGA 1.78 g

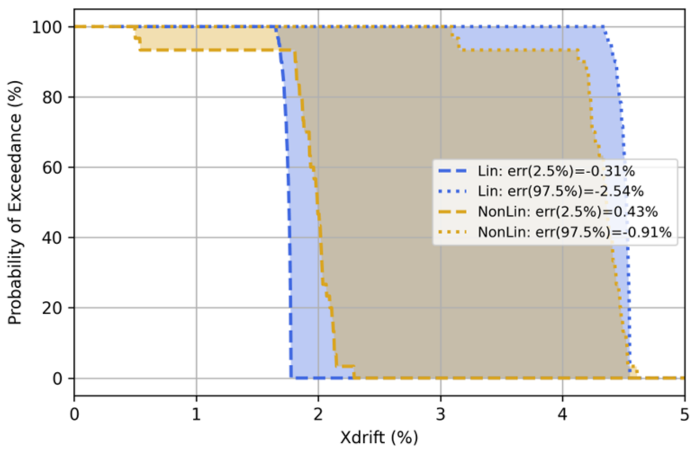

Figure 12. Corrected p-boxes for the linear and nonlinear models of SMART2013 at PGA 1.78 g

CONCLUSIONS AND PERSPECTIVES

This paper covers the issue of model validation for the purpose of safety margins assessment. By extension of the work of Roy and Oberkampf (2011), this paper proposes a new validation metrics that allows a clear distinction of the areas where the model predicts well reference data and the area of misfit, whether it is an overestimation of an underestimation, that cannot be explained by all uncertainties accounted for. The new metrics is itself expressed in terms of a cumulative distribution function that allows for the definition of a confidence interval that is not symmetric on both ends.

This new validation metrics is applied to the case of the SMART2013 RC building mock-up using both linear and nonlinear modelling methods. For this case study, one is provided with the mock-up details, the general experimental design plan, the main hypotheses regarding finite elements modeling. A Morris' sensitivity analysis was achieved which led to the selection of only most influential inputs. Finally, the numerical campaign, i.e., the uncertainty propagation and the associated post-processing, have been carried out. Along the validation metrics quantification, the PGA was considered as the main IM and the longitudinal drift as the main EDP of interest.

One should note that the primary outcome of using validation metrics is not to conclude whether a model is validated or not; as the question of what is the acceptable margin error remains a subjective one. One should rather see it as a tool to assess known uncertainties and give an insight on ways to improve the modeling (minimizing the error over the space of EDP range of interest). It could be by the reduction of input uncertainties, collection of additional experimental data closer to the conditions of interest or physical improvement in the model formulation. Also, it should be emphasized that the outcome of the validation process highly depends on the EDP and IM chosen. For instance, a mechanical model might perform well in predicting the structural drift while failing at providing an acceptable estimate of the floor response spectra. Similarly, other IM than the PGA, such as the relative average spectral acceleration (ASA40) proposed by De Biasio et al. (2014), might be more suitable for predicting the EDP output of the model.

Future research shall explore the coupling of metrics validation calculation and Bayesian updating techniques in order to account for reference data base enrichment. This could involve adjusting key inputs uncertainties or accounting for initial states that are not present in the default models. While this strategy seems promising, it would require careful consideration, additional programming, and confidence in the numerical model's robustness. Furthermore, investigating different numerical models or concrete constitutive relations might reveal new insights into achieving more accurate predictions for various EDPs.

REFERENCES

Baudin, M., Dutfoy, A., Iooss, B., and Popelin, A. (2016). "OpenTURNS: An Industrial Software for Uncertainty Quantification in Simulation," *Handbook of Uncertainty Quantification*, 1-38, Springer.

CEA (2022). Cast3M website: http://www-cast3m.cea.fr/.

De Biasio, M., Grange, S., Dufour, F., Allain, F., Petre-Lazar, I. (2014). "A simple and efficient intensity measure accounting for non-linear behavior of structures," *Earthquake Spectra*, 30(4), 1403-1426.

Herman, J. D., Kollat, J. B., Reed, P. M., and Wagener, T. (2013). "Method of Morris effectively reduces the computational demands of global sensitivity analysis for distributed watershed models," *Hydrology and Earth System Sciences*, 17(7), 2893-2903.

Langlade, T., Heitz, T., Courtois, A. and Voldoire, F. (2022). "Validation and verification of nonlinear mechanical models for nuclear buildings and equipment: an application," *Proc., SMiRT-26*, Berlin/Potsdam, Germany, July 10-15, 2022.

Richard, B., Ragueneau F., (2012). "Continuum damage mechanics-based model for quasi-brittle materials subjected to cyclic loadings: formulation, numerical implementation and applications," *Engineering Fracture Mechanics*, 98, 383-406.

Richard, B., Voldoire, F., Fontan, M., Mazars, J., Chaudat, T., Abouri, S. and Bonfils, N. (2018). "SMART 2013: Lessons learned from the international benchmark about the seismic margin assessment of nuclear RC buildings," *Engineering Structures*, 161, 207-222.

Roy, C. J. and Oberkampf, W. L. (2011). "A comprehensive framework for verification, validation, and uncertainty quantification in scientific computing," *Computer Methods in Applied Mechanics and Engineering*, 200(25-28), 2131-2144.